STUDY OF THE IODIDE–TRI-IODIDE REDOX ELECTRODE IN DIMETHYLSULPHOXIDE*

M. C. Giordano, J. C. Bazán and A. J. Arvía

Instituto Superior de Investigaciones, Facultad de Química y Farmacia,
Universidad de La Plata, La Plata, Argentina

Abstract—The electrochemistry of solutions of sodium iodide and sodium iodide with added iodine dissolved in dimethyl sulphoxide has been investigated in the temperature range from 25 to 45°C. The current voltage curves were determined using a platinum rotating disk electrode working at 300 up to 6000 rpm. Both anodic and cathodic processes were considered, in particular when solutions with added iodine were employed.

The anodic current/voltage curves are characterized by two well defined steps, the total limiting current being proportional to the iodide-ion concentration, while the cathodic current/voltage curve involves only one step, the limiting current density being linearly related to the tri-iodide-ion concentration.

From the diffusion-controlled processes, the diffusion coefficients of the diffusing species in both the cathodic and anodic processes were evaluated. The ratio between the diffusion coefficients of tri-iodide and those of the iodide ions is in agreement with the predictable values based on the results of the corresponding aqueous systems.

The current/voltage curves in the region before the limiting current densities are appreciably irreversible. Those curves were obtained by the method of Frumkin and Tedoradse for intermediate kinetics, and the kinetic parameters of the reactions, including the reaction orders, have been calculated. The kinetics of the reactions are discussed in terms of three possible reaction schemes which comprise the initial participation of iodide or tri-iodide ions. The experimental transfer coefficients for the cathodic and anodic processes add up to one.

Résumé—L'électrochimie des solutions d'iodure de sodium et d'iodure de sodium avec addition d'iode dissous dans du sulfoxyde diméthylique a été étudiée a des températures de 25° à 45°C. Les courbes courant/voltage ont été déterminées moyennant une électrode de platine à disque tournant à une vélocité de 300 à 6000 rpm. Les procéssus anodiques et cathodiques ont été examinés en particulier pour les solutions avec addition d'iode.

Les courbes courant/voltage sont caractérisées par deux vagues bien définies; le courant limite total est en proportion avec la concentration d'ions iodure, tandis que la densité du courant limite cathodique comprend une seule et accuse une relation linéaire avec la concentration d'ions de tri-iodure.

Les coefficients de diffusion de espèces diffusantes dans les procèssus anodiques et cathodiques furent déduits des procèssus controlés par la diffusion. Les rapports entre les coefficients de diffusion des ions de tri-iodure et ceux des ions d'iodure concordent avec les valeurs previsibles quant aux résultats des systèmes aqueux correspondants.

Les courbes courant/voltage dans la région antérieure aux densités de courant limite montrent un degré d'irréversibilité appréciable. Ces courbes ont été obtenues par la méthode de Frumkin et Tedoradse pour la cinétique des intermédiaires et les paramètres cinétiques des réactions, y compris l'ordre des réactions, ont été calculés. La cinétique des réactions se discute sur la base de trois schémas probables de réaction comportant chacun la participation initiale d'ions d'iodure ou de tri-iodure.

La somme des coefficients de transfer expérimentaux pour les procèssus cathodiques et anodiques est égale à un.

Zusammenfassung—Man untersuchte das elektrochemische Verhalten von Na-Iodid-Lösungen ohne und mit Iodzusatz in Methylsulfoxyd im Temperaturbereich zwischen 25 und 45°C. Stromspannungs-kurven wurden mittels einer rotierenden Scheibenelektrode aus Platin bei Rotationsgeschwindigkeiten zwischen 300 und 6000 Upm aufgenommen. Man untersuchte sowohl die anodischenals auch die kathodischen Reaktionen speziell bei Iodzusatz.

Die anodische Strom-Spannung Kurven unterscheiden sich durch zwei deutlich definierte Stufen und der Gesamtgrenzstrom steht im Verhältnis zu der Jodidionkonzentration während die kathodische Strom-Spannung-Kurve nur eine Stufe umfasst und die Grenzstromdichte ein Linearverhältnis zur Trijodidionkonzentration aufweist.

Aus den Vorgängen welche von der Diffusion bestimmt werden wurden die Duffusionskoeffizienten der Diffusorsubstanzen in den kathodischen und anodischen Vorgängen abgeleitet. Das Verhältnis zwischen dem Diffusionskoeffizienten des Trijodids und jenem der Jodidione stimmt mit der Vorhersoige auf Grund der Ergebnisse des entsprechenden wässerigen Systems überein.

Die Strom-Spannung-Kurven im Gebiet vor den Grenzstromdichten weisen einen bedeutenden Grad von Irreversibilität auf. Diese Kurven wurden mittels der Frumkin und Tedoradse Methode für Intermediärkinetik gewonnen und die kinetischen Parameter der Reaktionen mit Einbegriff der Reaktionsordmungen, wurde errechnet. Die Kinetik der Reaktionen wird an Hand von drei wahrscheinlichen Reaktionsschemen, welche den Anfangsanteil des Jodid- und Trijodidions mitumfassen, auseinandergesetzt.

Der Gesamtbetrag der experimentellen Uebertragungskoeffizgienten für die kathodischen und anodischen Vorgänge ist gleich eins.

INTRODUCTION

A previous study of the electro-oxidation of iodide ions in dimethylsulphoxide DMSO,[1] has shown that the anodic reaction comprises two definite steps in the current/voltage curve. Recently, the electrochemical behaviour of sodium iodide solutions with added iodine has been reported.[2] These solutions exhibit only one cathodic step. It was found that the relative height of the anodic steps depends on the ratio of iodine to iodide present in the solution. While the first anodic wave increases with iodide-ion concentration, the second anodic wave does go with tri-iodide-ion concentration. The existence of the couple iodide/tri-iodide in the solutions suggested the possibility of a full study of the electrochemical process as involved in both the anodic and cathodic electrode reactions.

In the course of the study attempted in consequence, suitable reference electrodes were found for these ionic media. We also attempted to elucidate the kinetics of the preceding reactions, because a previous chronopotentiometric study[3] had indicated the existence of an appreciable activation polarization when the electrolysis is performed in a region prior to the limiting current density.

To prove the existence of this irreversibility, the electrochemical reaction was studied on a platinum rotating disk electrode, over a wide range of experimental conditions.

EXPERIMENTAL TECHNIQUE

1. *Electrolysis cells*

Two electrolysis cells were used; both were designed according to the hydrodynamic requirements involved in the application of the rotating disk electrode technique. One of the cells consisted of a glass container of about 100 ml capacity and the other had separated cathodic and anodic sections connected by means of a stopcock lubricated with the same solution. Both were completed with the rotating disk electrode, the counterelectrode and the reference electrode, properly placed. Two platinum rotating disks were indiscriminately used. One of these was embedded in a Lucite rod and the other was fixed into a Pyrex glass rod. The diameter of the working electrodes in both cases was about 3 mm and the external diameter of the rotating rod was about 1 cm. The disk electrode was symmetrically placed in the cell, and the capillary tip of the reference electrode was placed at one side of the rotating disk to avoid as far as possible any perturbation in the liquid flow. The working electrodes were polished to a mirror surface and activated with cathodic pulses either in acid solutions or in the same solutions used for the electrolysis. Except for

minor details and improvements in the electrical contacts as well as other mechanical features, the experimental set-up was similar to that described previously.[4]

The electrodes were rotated by means of a specially designed electronic rotator, with automatic compensation for the rotating couple.[5] The rotation speed was varied from 300 to 6000 rpm and was read by means of a stroboscope for the lower speeds and electronically for the higher. Further details about instrumentation are described elsewhere.[6] The electrolysis cells were completely tight and provided with inlet and outlet tubes to maintain a controlled atmosphere into the cell and to remove any trace of oxygen dissolved in the solutions.

The cells were placed into a double wall container which was filled with distilled water. Temperature was controlled with a Haake ultra-thermostat provided with a circulatory pump.

2. Solutions

Solutions were carefully prepared from previously purified AR quality chemicals and highly purified DMSO as solvent, as described previously[2] under a dry nitrogen atmosphere avoiding any contact with air.

TABLE 1

C_{NaI} M	C_{I_2} M	C_{KClO_4} M	Temp °C	δ g/cm^3	$\nu \times 10^2$ cm^2/s
0·03870	—	0·861	25·0	1·148	3·199
0·00348	—	0·764	25·0	1·153	3·006
0·00776	—	0·694	25·2	1·149	2·877
			34·0	1·137	2·331
			42·3	1·126	1·976
0·0407	0·0219	0·805	25·0	1·165	3·188
			35·0	1·154	2·576
			44·6	1·145	2·153
0·0406	0·0041	0·805	25·0	1·161	3·172
			34·5	1·151	2·573
			42·5	1·140	2·150
0·0402	0·0016	0·801	25·0	1·160	3·185
			32·9	1·150	2·539
			41·9	1·140	2·137

The iodide concentration was varied from 5×10^{-4} M to 5×10^{-2} M. Iodine concentration covered the range from 2×10^{-2} M to 2×10^{-4} M. In the solutions where iodine was added the concentration ratio between sodium iodide and iodine was changed from 2 to 40 or thereabouts. Sodium perchlorate was employed as the supporting electrolyte at a concentration of about 0·8 M, which was the largest advisable concentration to be employed because of the solubility of the salt in DMSO.[7]

The concentrations of the solutions were evaluated by potentiometric titration using conventional methods. Their viscosity and density were determined in the usual way; these data are assembled in Table 1. Solutions were studied for the temperature range from $25·0 \pm 0·1$ to $45·0 \pm 0·1°C$.

RESULTS

The current/voltage curves were obtained at different speeds of rotation, either by increasing or decreasing the speed of rotation. An interval of about 15 min was

allowed between consecutive determinations in order to let the solution recover its full homogeneity and the working electrode attain its initial potential. These details were observed to get a satisfactory reproducibility in the current/voltage curves and to avoid hysteresis, which occurred when the above mentioned precautions were disregarded. The current/voltage curves were thus obtained starting from the initial equilibrium potential and each point was read when both the current and the potential had attained steady values.

The current/voltage curves shown in Figs. 1–6 correspond to cathodic and anodic reactions under different experimental conditions.
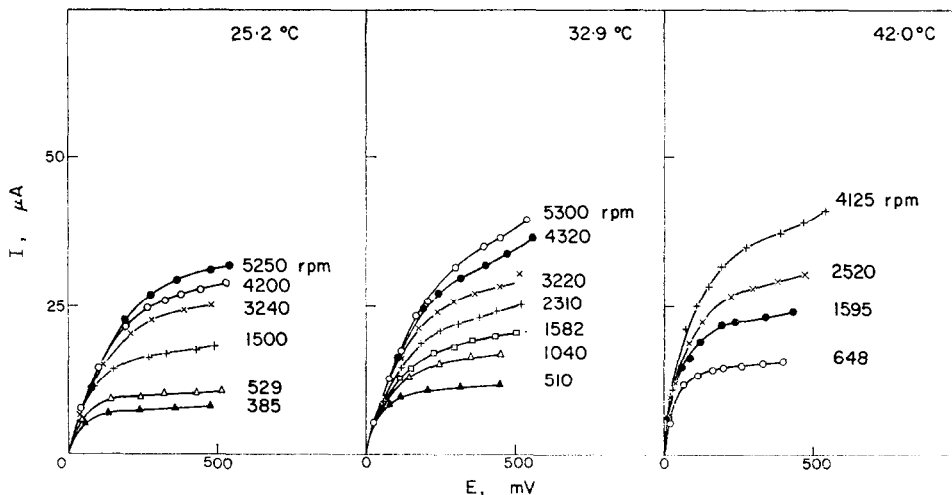

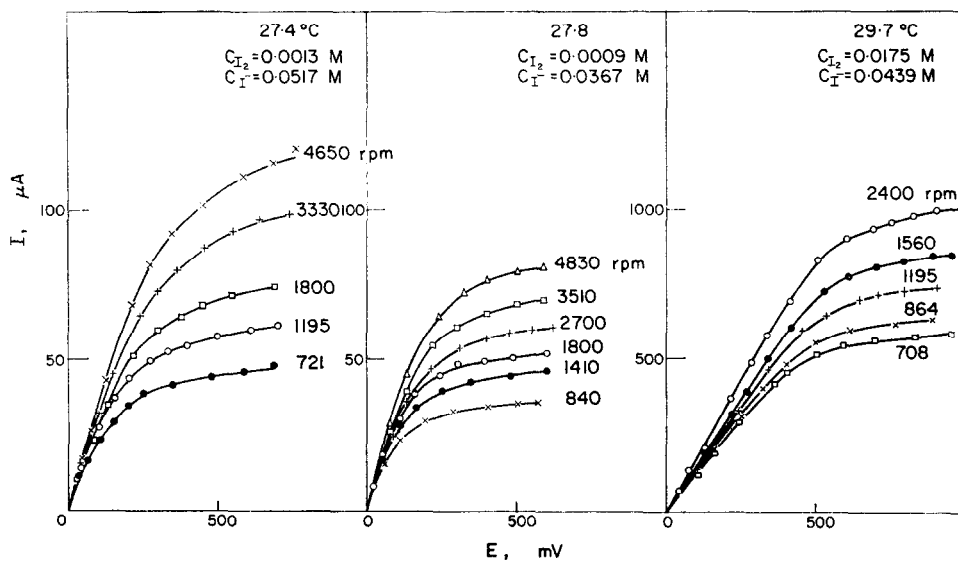FIG. 1. Cathode current/voltage curves.
$C_{I_2} = 0.0016$ M; $C_{NaI} = 0.0402$ M.

FIG. 2. Cathode current/voltage curves.
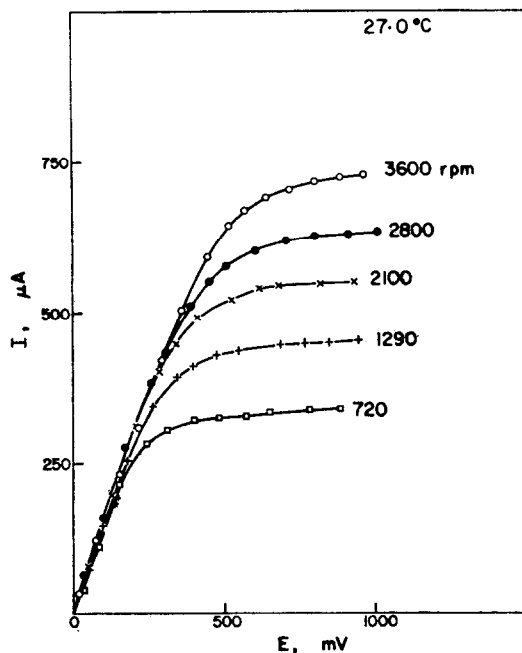
FIG. 3. Cathode current/voltage curves.
$C_{I_2} = 0.0105$ M; $C_{NaI} = 0.0615$ M.
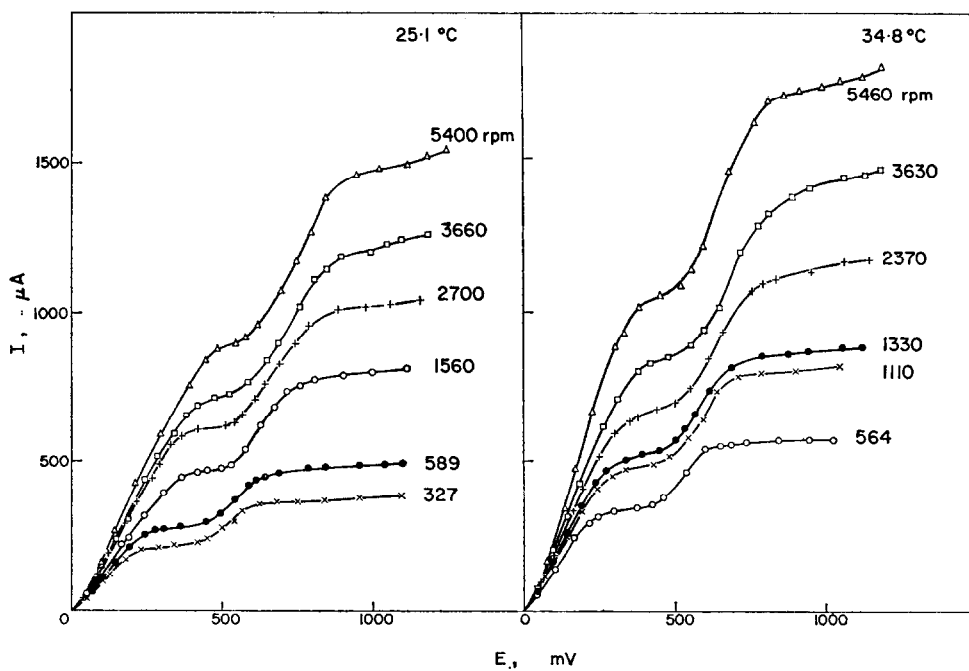

FIG. 4. Anode current/voltage curves.
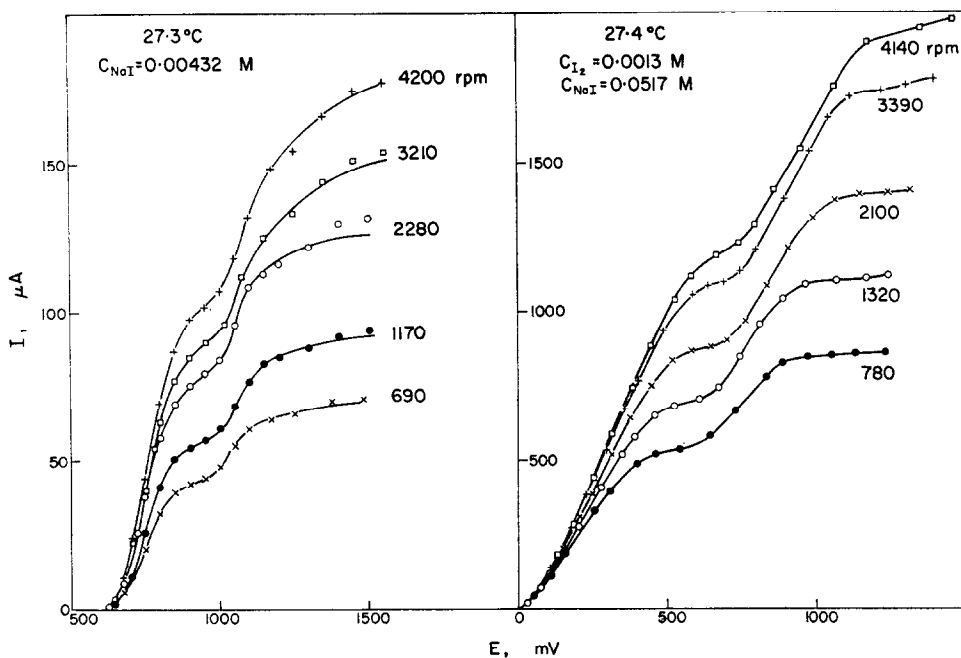$C_{I_2} = 0.00411$ M; $C_{NaI} = 0.00406$ M.

2

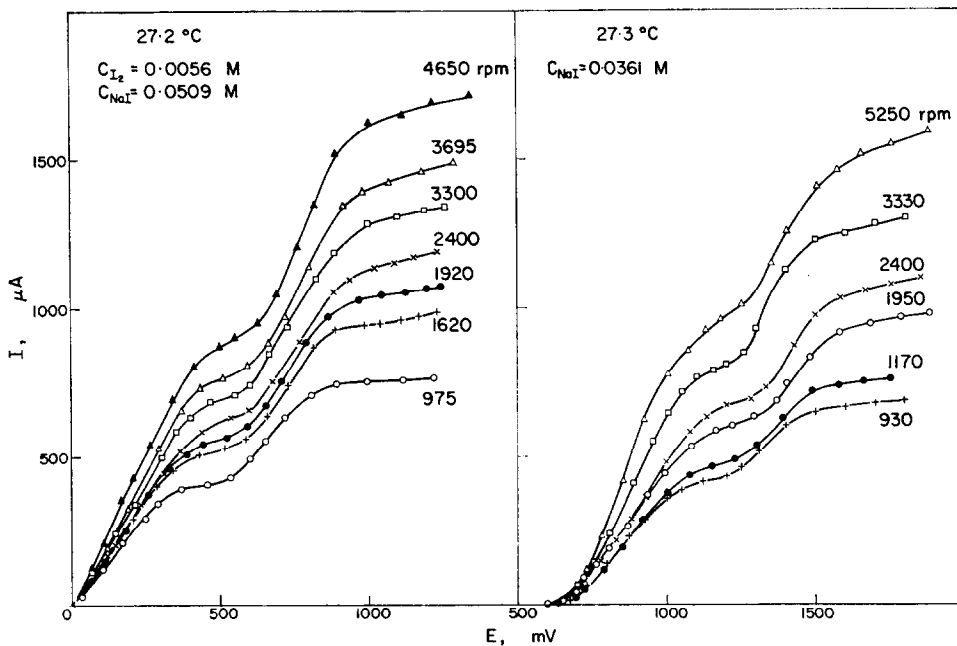FIG. 5. Anode current/voltage curves.

FIG. 6. Anode current/voltage curves.

INTERPRETATION AND DISCUSSION

1. *Electrochemical processes associated with the cathodic and anodic waves*

The interaction between iodine and DMSO as studied spectrometrically,[8,9] originates, under certain conditions, the formation of tri-iodide ions in the solution where no iodide ions were present before. Independently, as the anodic reaction yields tri-iodide ions, the following equilibrium must be taken into account in the electrode process investigated here,

$$I^- + I_2 \rightleftharpoons I_3^-. \tag{I}$$

Previous studies[2] have also indicated that the equilibrium reaction tends towards tri-iodide formation, and have suggested that the limiting current densities are related to the ionic species involved in reaction (I).

The limiting current densities referred to the apparent electrode area were plotted as a function of the square root of the rotation speed yielding satisfactory straight lines, as shown in Figs. 7–9, according to the theory of the rotating disk electrode.[10]

When using sodium iodide solutions a reversible initial potential was observed between the working electrode and the silver/silver-iodide reference electrode, after the electrode had been used as anode for a short time. This emf was about 600 mV. The following equilibria will be assumed to interpret the above mentioned figure,
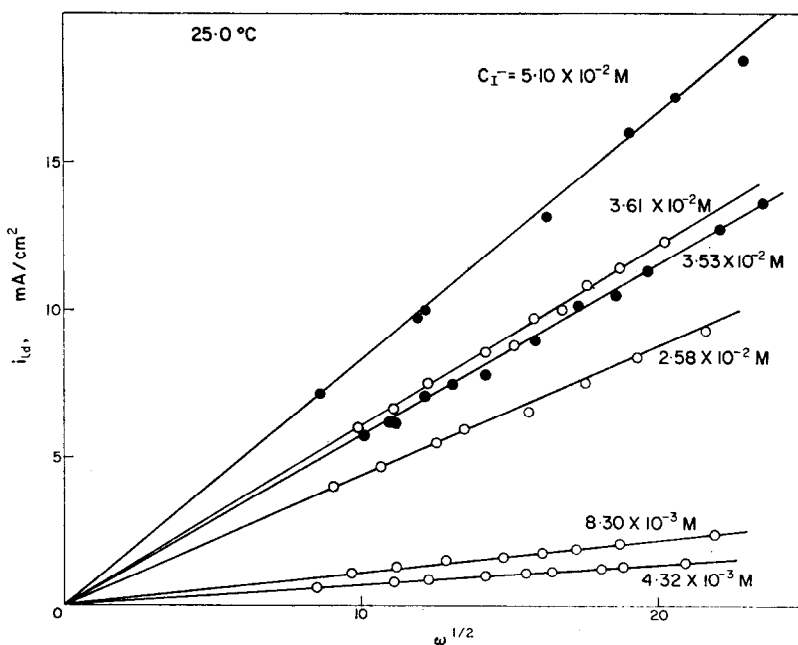
$$AgI + e = Ag + I^-, \tag{IIa}$$

$$I_3^- + 2e = 3I^-. \tag{IIb}$$
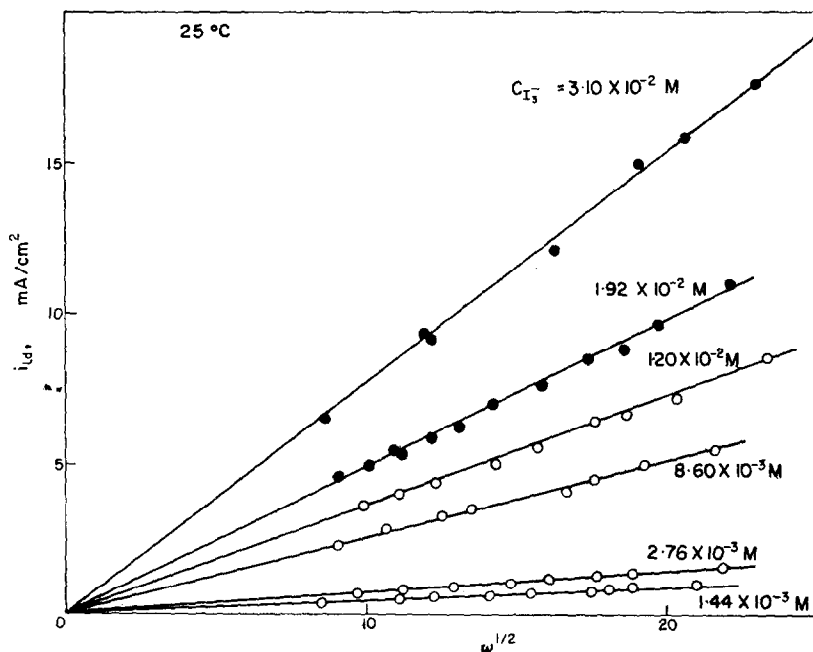

FIG. 7. Dependence of the first anodic limiting current density on the rotation speed.
O; NaI solutions; ●; NaI solutions with added I_2.

FIG. 8. Dependence of the second anodic limiting current density on the rotation speed.
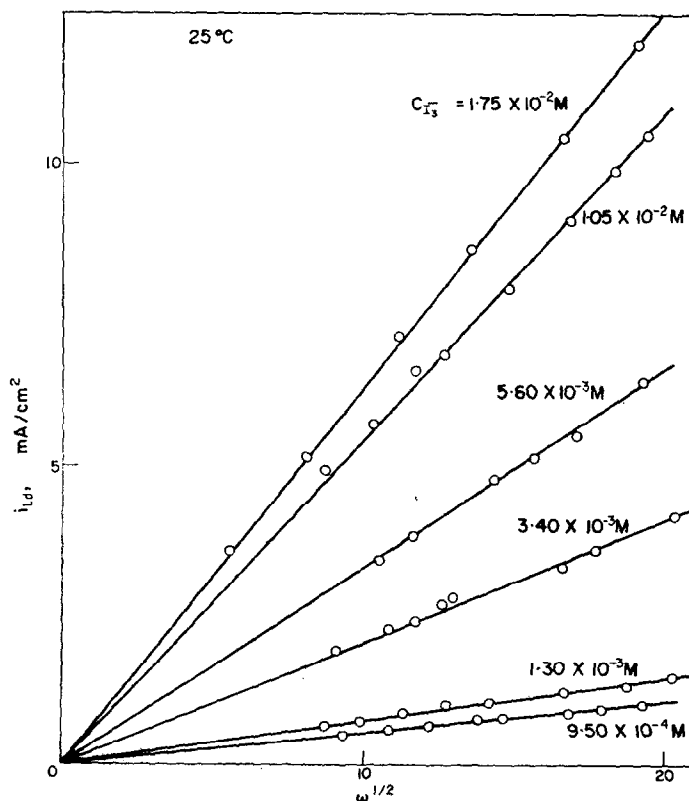$\bigcirc$; NaI solutions; $\bullet$; NaI solutions with added I_2.

FIG. 9. Dependence of the cathodic limiting current density on the rotation speed.

To calculate the values of the emf found with the different solutions on the basis of IIa and IIb we take into account the initial iodide-ion concentration and the amount of tri-iodide ion formed during the duration of the electrolysis. The Nernst equations for reactions IIa and IIb, respectively, are

$$E_{\text{IIa}} = E_{\text{IIa}}^{\circ} + \frac{RT}{F} \ln \frac{1}{a_{\text{I}^-}} \tag{1}$$

and

$$E_{\text{IIb}} = E_{\text{IIb}}^{\circ} + \frac{RT}{2F} \ln \frac{a_{\text{I}_3^-}}{(a_{\text{I}^-})^3}. \tag{2}$$

To apply these equations, E_{IIa}° and E_{IIb}° are taken as equal to the standard potentials of the corresponding aqueous equilibria. Although this assumption is not strictly true for the individual values of the electrode potentials because of their dependence on the dielectric constant of the solvent, the error in their difference, which is actually the significant figure in the present case, should not be appreciable as compared to that in the experimental results. Taken at 25°C, $E_{\text{IIa}}^{\circ} = -0.152$ V and $E_{\text{IIb}}^{\circ} = 0.537$ V;[11] the calculated values of emf of the reversible cell left after the electrolysis, which are assembled in Table 2, are thus in agreement with the experimental values, at least for the more dilute solutions.

TABLE 2

C_{I^-} M	Temp °C	(Emf)$_{\text{exp}}$ mV	(Emf)$_{\text{cal}}$ mV
0·00432	27·2	630 ± 10	631
0·00770	25·0	590	601
0·00830	27·2	600	594

The foregoing arguments may be used to predict the order in which electrochemical reactions should occur on the working electrode with an increasing or decreasing potential, according to the redox potential of the different couples, already mentioned. From the Nernst equations the following conclusions are drawn. Apart from equilibrium II, iodide ion can participate also in the following different redox process, which is clearly related to the former,

$$I_2 + 2e = 2I^-. \tag{III}$$

Its redox potential is given by

$$E_{\text{III}} = E_{\text{III}}^{\circ} + \frac{RT}{2F} \ln \frac{a_{\text{I}_2}}{(a_{\text{I}^-})^2} \tag{3}$$

where, as before, we take $E_{\text{III}}^{\circ} = 0.620$ V.

If the iodine concentration is smaller than any iodine or tri-iodide ion concentrations, as earlier suggested on the basis of structural and solubility studies,[12] $E_{\text{III}} < E_{\text{IIb}}$, and at lower anodic potentials the oxidation of iodide ion should occur preferentially via reaction III and equilibrium I, assuming a fast reaction. The direct oxidation of tri-iodide ion should occur at a higher potential and this process might in principle be responsible for the second step in the anodic current/voltage curve.

The same explanation obtains for the only cathodic wave observed in the case of

solutions added with iodine. If the latter is assumed to exist preferentially as tri-iodide ion, it will react in the cathode at lower potentials.

From the analysis of the electrode potentials therefore, we conclude that the overall reaction is related to the reduction of tri-iodide ion at the cathode and the oxidation of iodide and tri-iodide ions at the anode, these ions being respectively related to the first and second anodic waves. Consequently, the cathodic limiting current density should be proportional to tri-iodide-ion concentration, while the sum of the limiting current density observed in the two anodic steps should be proportional to the iodide-ion concentration. Results shown in Fig. 10 indicate that the linear dependence of limiting current densities on concentrations supports with the above assumptions.
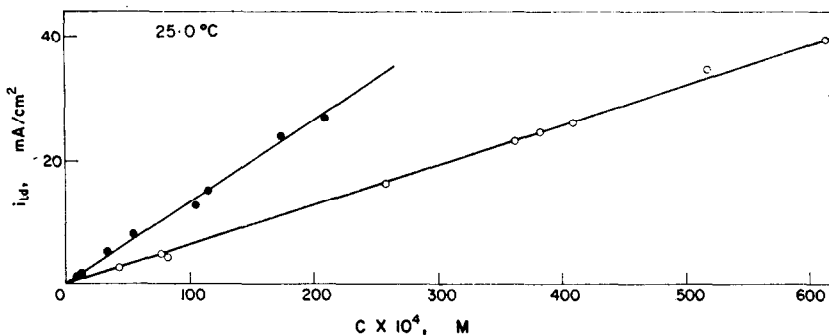

FIG. 10. Dependence of the limiting current density on concentration.
O, total anodic limiting current density *vs* iodide-ion concentration; ●, cathodic limiting current density *vs* iodine concentration.

2. *The diffusion coefficients of reacting species*

As indicated by the dependence of the limiting current density on the square root of rotation speed, the electrode processes are, under these circumstances, convective-diffusion controlled. Hence, the diffusion coefficient of the reacting species can be evaluated from the limiting current densities by means of the equation for the rotating disk electrode as given by Levich,[10]

$$i_{\mathrm{ld}} = \frac{zFD_i^{2/3}\omega^{1/2}C_0}{1 \cdot 61 \, \nu^{1/6}}. \tag{4}$$

D_i is the experimental diffusion coefficient of ion i, C_0 is the concentration of the reacting species in the bulk of the solution, ν is the kinematic viscosity, ω is the speed of rotation, i_{ld} is the limiting current density and z is the number of electrons associated with one mole of the diffusing ion.

To interpret the meaning of the diffusion coefficients obtained from the cathodic and anodic waves, let X be the concentration of iodine added to the solution and C_0 the initial concentration of iodide ion. If the iodine concentration is lower than the iodide concentration and if equilibrium I is preferentially shifted towards tri-iodide ion formation, the limiting current densities for each ion are respectively

$$(i_{\mathrm{ld}})_{\mathrm{I}^-} = k_{\mathrm{I}^-}(1 - X)C_0 \tag{5}$$

and

$$(i_{\mathrm{ld}})_{\mathrm{I}_3^-} = k_{\mathrm{I}_3^-}C_{\mathrm{I}_3^-} = k_{\mathrm{I}_3^-}XC_0, \tag{6}$$

where k_{I^-} and $k_{I_3^-}$ are the mass-transfer rate-constants. For the anodic reaction, if it is further assumed that $k_{I_3^-} \approx k_{I^-}$, we have

$$\Sigma(i_{ld})_a = (i_{ld})_{I_3^-} + (i_{ld})_{I_3^-} \approx k_{I^-}C_0. \tag{7}$$

Therefore, the experimental diffusion coefficients obtained from the cathodic wave should correspond to tri-iodide ion, while the figure obtained from both anodic waves should correspond to a first approximation to iodide ion.

Values of the experimental diffusion coefficients of iodide and tri-iodide ions are shown in Table 3, and can immediately be compared with those determined in an

TABLE 3

Ionic species	$D \times 10^5$ cm²/s	Temp °C	Ionic medium	Reference
I_3^-	0·37	25·0	0·8 M $KClO_4$(DMSO)	This work
I^-	0·69	25·0	0·8 M $KClO_4$(DMSO)	This work
I_3^-	0·42	25·0	1·0 N H_2SO_4(aq)	(13)
I^-	0·81	25·0	1·0 N H_2SO_4(aq)	(13)
I_3^-	1·38	25·0	1·0 N H_2SO_4(aq) and	(14)
I^-	2·20	25·0	1·5 M IK(aq)	(14)
I_3^-	1·13	25·0	0·1 M IK(aq)	(15)

aqueous medium for the same ions, in spite of the divergence of results reported for the latter,[13–15] as shown in the data assembled in the same table. It is clear that in both media the diffusion coefficient of tri-iodide ion is smaller than the corresponding figure for the iodide ion. The ratios between them in both media are approximately the same, a reasonable result which can be predicted from the theories of viscosity and diffusivity.[16] Thus, if the value of D given recently[16] for aqueous solutions is taken as the more reliable one, then, at 298°K, we get

$$\left(\frac{D\eta}{T}\right)_{I_3^-(aq)} = 3·37 \times 10^{-10} \text{ g/cm}^3 \text{ °K}. \tag{8}$$

Under the same circumstances we have for the DMSO solutions, neglecting any correction for ionic strength,

$$\left(\frac{D\eta}{T}\right)_{I_3^-(DMSO)} = 4·31 \times 10^{-10} \text{ g/cm}^3 \text{ °K}. \tag{9}$$

3. Departure from a pure convective-diffusion control

Although the limiting current densities indicate clearly a region where the reaction is actually under convective-diffusion control, the situation at lower current densities appears rather complicated. As a matter of fact, when the whole polarization curve is analysed a distortion from a pure concentration polarization becomes evident.

The higher the speed of rotation, the larger the distortion observed and the smaller the region of limiting current densities. The half-wave potentials, apart from being a function of the concentration of the reacting ion also depends on the rotation speed, and their difference, as in the case of the anodic waves, is also a function of the rotation rate. The observations drawn from current/voltage curves, suggest that the electrode processes under investigation involve, besides concentration polarization, a significative activation polarization contribution. Hence, to evaluate each contribution independently in relation with the kinetics of the reaction, experimental results were analysed following the method of Frumkin and Tedoradse[17] for electrode processes occurring on the rotating disk electrode with intermediate kinetics. Accordingly, for a particular run, data obtained at an overpotential η_k where the current is lower than the limiting current density i_k, should be considered. If i_L is the value of the limiting current density at a certain speed of rotation ω_0, the following equation results:

$$i_k = i_L \left[1 - \left(\frac{i_k}{i_L} \right)^{1/p} \right],$$
(10)

where p is the order of the electrode reaction. The latter can immediately be obtained from (10),

$$p = \frac{\log i_L - \log i_k}{\log i_L - \log (i_L - i_k)},$$
(11)

if i_L is known, and this is easily calculated if the reaction order is one. (10) can then be written

$$\frac{1}{i} = \frac{1}{i_L} + \frac{1}{A C_0 \omega^{1/2}}.$$
(12)

Results, according to (12), would furnish a straight line if $1/i$ is plotted against $1/\omega^{1/2}$ and its extrapolation at infinite rotation speed would yield the contribution of the
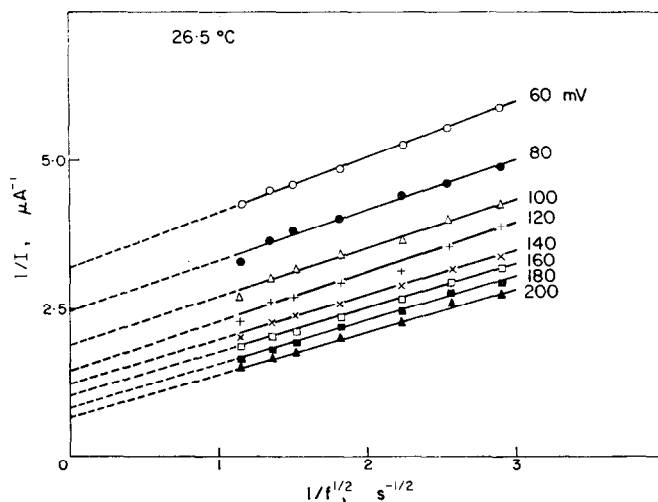

Fig. 11. Plot according to (12). Cathodic waves.
f, rotation frequency of the working electrode; C_{I_2}, 0·0013 M; C_{NaI}, 0·0517 M.
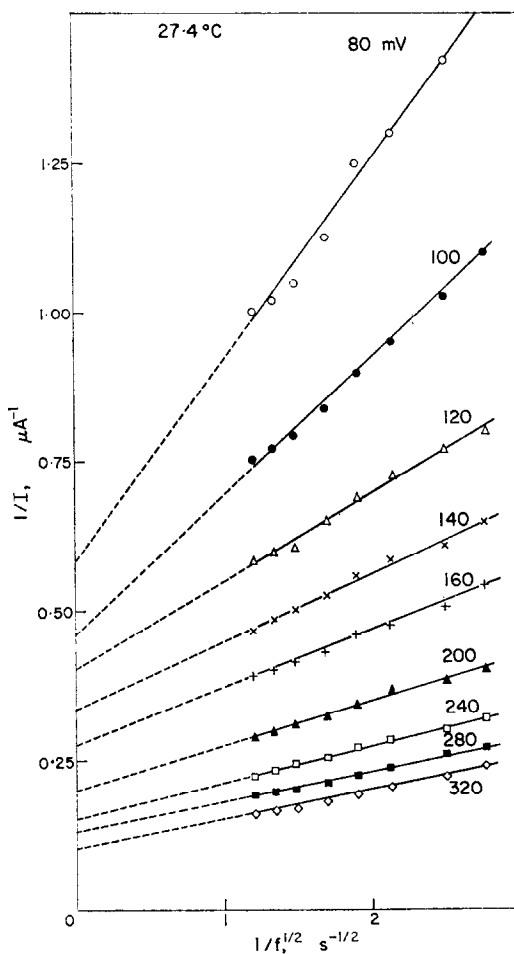
FIG. 12. Plot according to (12). First anodic wave $C_{I_2} = 0.0013$ M; $C_{NaI} = 0.0517$ M.

activation polarization. Nevertheless, under certain circumstances this procedure can involve a pseudo-ohmic polarization term, η_r, included in the extrapolated figure. The latter is insignificant in aqueous systems at high ionic concentration, but this is not the case here. Hence, to evaluate the contribution of the actual activation polarization another correction of the extrapolated value, calculated as described further on, is also required. Results plotted according to (12) are shown in Figs. 11 to 13. Therefore in a general case the overpotential related to i_L, assuming that η_a follows the Tafel law, is

$$\eta_r = \eta_a + \eta_r = a + b' \ln I_L + I_L R, \tag{13}$$

where the η's are the different polarization terms, a and b' are Tafel constants, I_L is the extrapolated current and R the ohmic resistance between the working electrode and the reference electrode.

To evaluate R and in order to separate η_a from η_r, we derive (13) as follows,

$$\frac{\partial \eta_r}{\partial I_L} = \frac{b'}{I_L} + R, \tag{14}$$

where $b' = b/2 \cdot 303$. Then, by plotting $\partial \eta_r / \partial I_L$ vs $1/I_L$, R can be estimated as indicated in Figs. 14 and 15. The value of R is in the present case about 30 Ω. This figure,
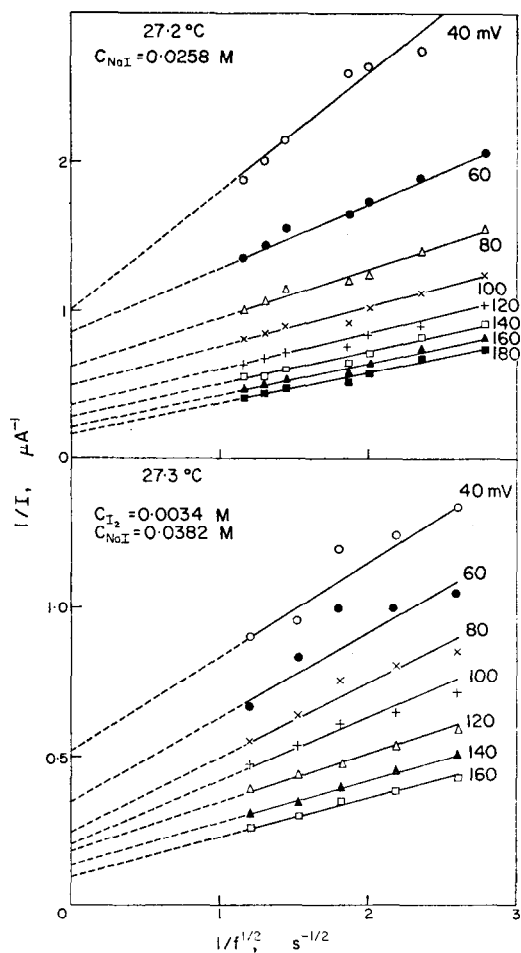

Fig. 13. Plot according to (12). Second anodic wave.

although high at first sight, is not unreasonable if we take into account the cell design and the conductivity of DMSO solutions.[7] The value of R was also confirmed by means of independent measurements.[18] The actual η_a was now calculated and plotted according to a Tafel equation. The results for the cathodic and for the first wave of the anodic runs are shown in Figs. 16 and 17.

A further complication arises with the portion of the current/voltage curve belonging to the second anodic wave, because it is necessary to fix the starting

potential associated with it. From the current/voltage curves properly corrected for the ohmic drop, the initial potential of the second wave was graphically obtained by an interpolation of the two plateau with the ascending branch of the second anodic
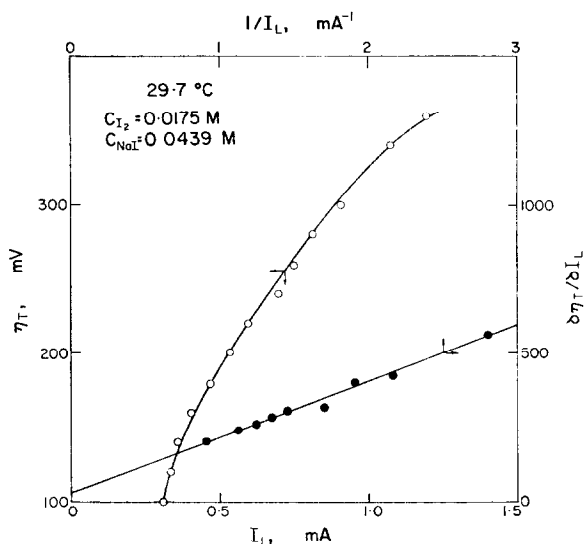

FIG. 14. Evaluation of η_r, according to (14), from the cathodic waves.

wave. After that, the same procedure already described was followed. Results for the second anodic wave are shown in Fig. 18.

From the Tafel plots, the parameters b, i_0 and α were calculated as usual, and they are assembled in Table 4. The reaction order with respect to each initial reacting
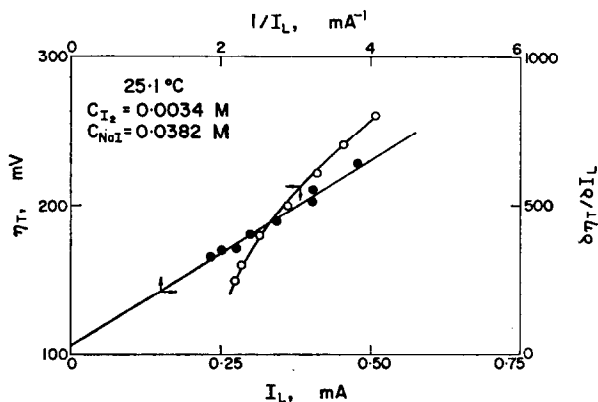
FIG. 15. Evaluation of η_r, according to (14), from the first anodic wave.

species was calculated from (11), since i_k is obtained immediately if i_L is known. By plotting the limiting diffusional current density and the current density i, at a value of η_k lower than that corresponding to i_{ld}, against the square root of the rotation speed, the results given in Figs. 19 and 20 are obtained. There the straight line
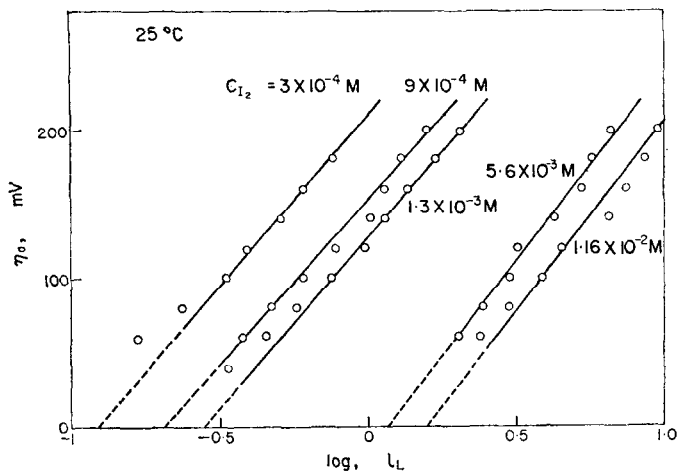
Fig. 16. Tafel plots from the cathodic waves.
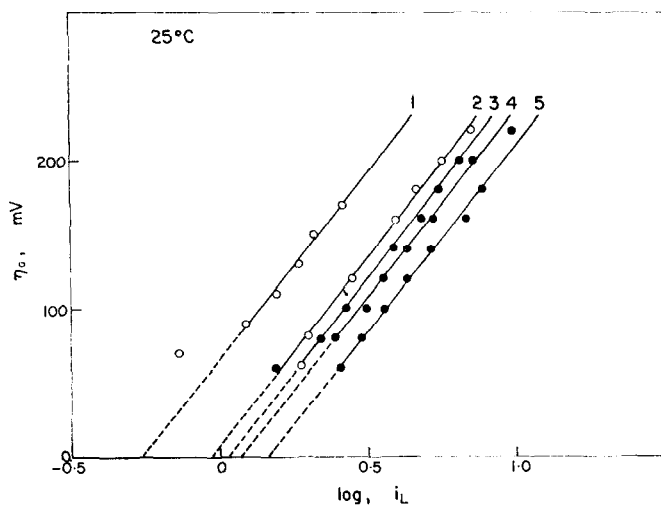
Fig. 17. Tafel plots from the first anodic waves.
1, C_{NaI}, $8\cdot3 \times 10^{-2}$M;
2, C_{NaI}, $2\cdot58 \times 10^{-2}$M;
3, C_{NaI}, $3\cdot82 \times 10^{-2}$M; C_{I_2}, $3\cdot4 \times 10^{-2}$M;
4, C_{NaI}, $5\cdot17 \times 10^{-2}$M; C_{I_2}, $1\cdot3 \times 10^{-2}$M;
5, C_{NaI}, $4\cdot09 \times 10^{-2}$M; C_{I_2}, $5\cdot6 \times 10^{-2}$M.
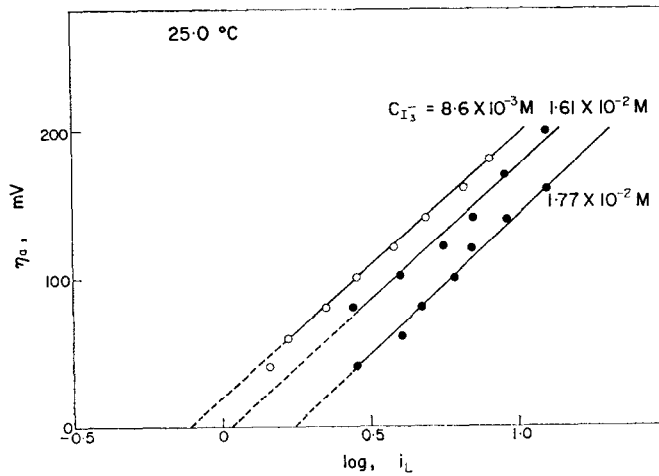
Fig. 18. Tafel plots from the second anodic waves.

TABLE 4. KINETIC PARAMETERS

Cathodic reaction C_{I_2} M	Temp °C	P	b_c mV	$(i_0)_c$ mA/cm^2	α
0·0175	29·7	0·98	250	1·59	0·24
0·0116	26·8	1·01	230	1·23	0·26
0·0105	27·0	0·82	250	1·17	0·24
0·0056	27·2	1·00	250	1·13	0·24
0·0022	24·9	0·98	220	0·28	0·27
0·0013	27·4	1·18	230	0·29	0·26
0·0009	27·8	1·06	230	0·38	0·26
0·0003	25·0	0·95	230	0·09	0·26

Anodic reaction (1) C_{I^-} M	Temp °C	P	$(b_1)_a$ mV	$(i_{0,1})_a$ mA/cm^2	$(\alpha_1)_a$
0·0510	26·7	0·92	220	1·36	0·27
0·0504	29·5	1·01	215	1·30	0·27
0·0370	25·0	1·00	220	0·76	0·27
0·0353	27·2	1·15	230	1·14	0·26
0·0348	27·3	0·97	250	1·19	0·24
0·0340	25·1	1·00	200	1·43	0·30
0·0278	27·3	1·04	250	0·87	0·24
0·0074	27·2	1·00	200	0·38	0·30

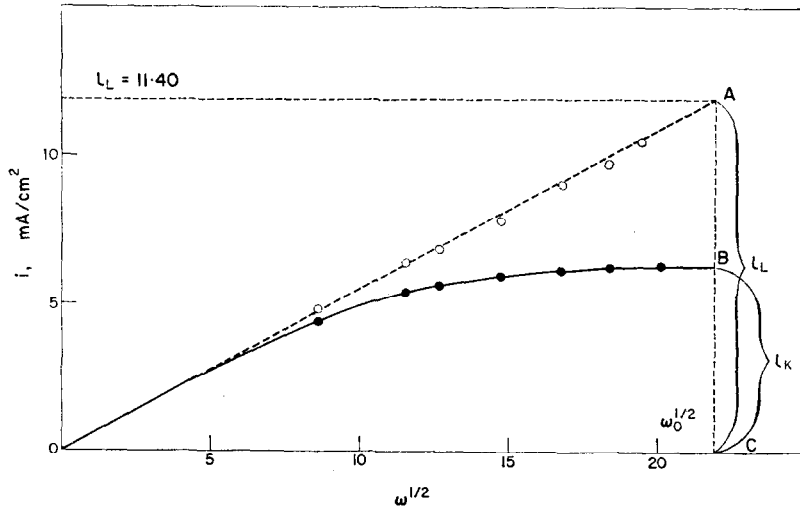| Anodic reaction (2) $C_{I_3^-}$ M	Temp. °C	P	$(b_2)_a$ mV	$(i_{0,2})_a$ mA/cm^2	$(\alpha_2)_a$
0·0310	27·0	0·98	130	0·80	0·46
0·0192	27·2	1·05	120	1·43	0·50
0·0185	27·8	1·00	120	1·43	0·50
0·0161	28·0	1·00	140	0·60	0·43
0·0120	27·3	1·00	120	1·29	0·50
0·0028	27·2	1·00	120	0·11	0·50
0·0025	25·2	1·00	120	0·16	0·50

FIG. 19. Dependence of cathodic current density on $\omega^{1/2}$.
$\bigcirc$, limiting current density: $\bullet$, current density at $\eta_k = 300$ mV; C_{I_2}, 0·0105 M; C_{NaI}, 0·0615 M; 25°C.
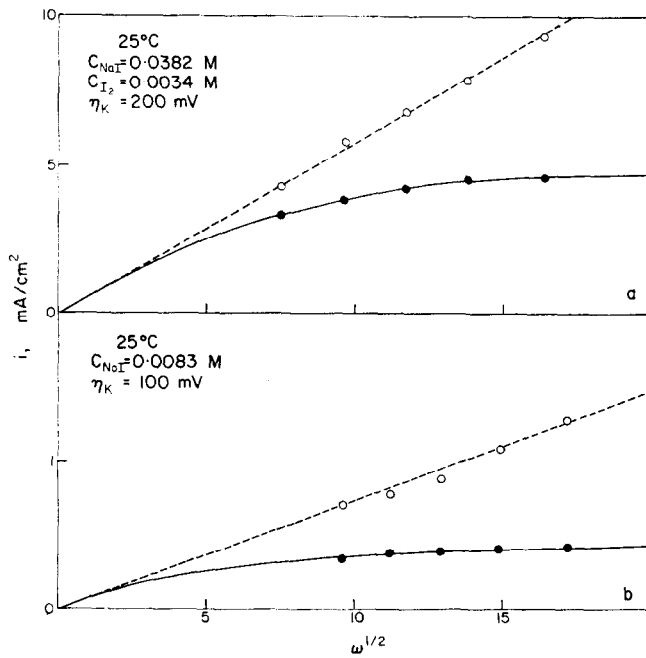

FIG. 20. Dependence of the anodic current on $\omega^{1/2}$.
a: data from the first wave; b: data from the second wave.

corresponds to Levich's equation for the rotating disk electrode and the initial slope of the former curve approaches that of the latter. According to the definition given above, the value of i_L corresponds in the straight line to a value of $\omega^{1/2} = \omega_0^{1/2}$ and is related to the value of i_k on the curve. From those plots the following relationship is drawn:

$$p = \frac{\log \dfrac{AC}{BC}}{\log \dfrac{AC}{AB}}. \tag{15}$$

Values of p obtained from (15) are also included in Table 4. There the C_i's refer to the molar concentration of species i, subscripts c and a indicate cathodic and anodic parameters and subscripts 1 and 2, refer to the first and second anodic waves respectively. The estimated error for i_0 resulting from a $\log i_0$ vs $\log C$ plot is of the order of 30%. This error is due to the various extrapolations and corrections involved in its calculation.

The experimental activation energies were obtained from the temperature dependence of i_0 and are assembled in Table 5 together with the experimental activation energies for the diffusional processes, as resulting from the temperature dependence of the limiting current densities.

TABLE 5. EXPERIMENTAL ACTIVATION ENERGIES

From $\log i_0$ vs $1/T$	
	$(E_a)_c = 4000 \pm 500$ cal/mol
	$(E_{a_1})_a = 4000 \pm 500$ cal/mol
	$(E_{a_2})_a = 3000 \pm 500$ cal/mol
From $\log i_{ld}$ vs $1/T$	
	$(E'_a)_c = 3100 \pm 500$ cal/mol
	$(E'_{a_1})_a = 2980 \pm 500$ cal/mol
	$(E'_{a_2})_a = 3700 \pm 500$ cal/mol

4. Theoretical reaction paths related to the iodide–tri-iodide–iodine redox system

The analysis of current/voltage curves indicates the existence of a certain irreversibility in the redox electrode processes at overpotentials lower than those corresponding to the limiting current density. This effect was also observed in the chronopotentiometric study of the same reaction.[3]

The analysis and interpretation of results allow the evaluation of the irreversibility contribution to the electrode reaction, so we are now able to find out which are the most likely reactions responsible for the activation overpotential.

In order to establish a reaction scheme for each electrode process we should keep in mind that iodide and tri-iodide ions and iodine are the entities which must participate in the initial electrode reaction and that the concentration of the latter under the present experimental conditions is actually low.

Let us consider then the following three reaction schemes:

$$\text{(I)} \begin{cases} \text{I}^- + \text{M} \rightleftharpoons \text{M (I)} + \text{e} & \text{(I-1)} \\ \text{M(I)} + \text{M(I)} \rightleftharpoons 2\text{M} + \text{I}_2 & \text{(I-2)} \\ \text{I}_2 + \text{I}^- \rightleftharpoons \text{I}_3^-, & \text{(I-3)} \end{cases}$$

$$\text{(II)} \begin{cases} \text{I}^- + \text{M} \rightleftharpoons \text{M(I)} + \text{e} & \text{(II-1)} \\ \text{M(I)} + \text{I}^- \rightleftharpoons \text{I}_2 + \text{M} + \text{e} & \text{(II-2)} \\ \text{I}_2 + \text{I}^- \rightleftharpoons \text{I}_3^- & \text{(II-3)} \end{cases}$$

and

$$\text{(III)} \begin{cases} \text{I}^- + \text{M} \rightleftharpoons \text{M(I)} + \text{e} & \text{(III-1)} \\ \text{M(I)} + 2\text{I}^- \rightleftharpoons \text{I}_3^- + \text{M} + \text{e}. & \text{(III-2)} \end{cases}$$
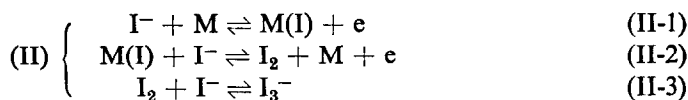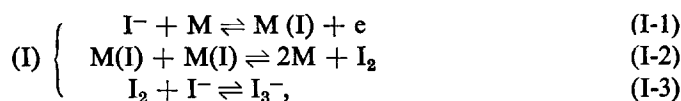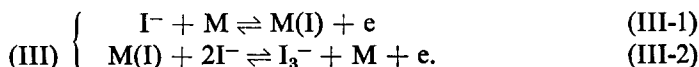
In these reactions, M is an active reaction site on the platinum electrode and M(I) an iodine atom on the electrode surface. Assuming that we are dealing with a consecutive scheme of reactions, there are several possibilities for the kinetics of the electrode process, since each step might in principle become rate-determining. Formally each of these possibilities can be accounted for in the same way as for the kinetics of the hydrogen electrode,[19] assuming in the simplest case that the surface coverage is relatively low and a Langmuir adsorption is obeyed.

In this case, a quasi-steady state analysis yields the theoretical parameters presented in Table 6, where $\Delta\phi$ refers to the potential of the electrode/solution interphase and

TABLE 6

Rate-determining step	$\dfrac{RT}{F}\left(\dfrac{\partial \ln i_0}{\partial \Delta\phi_0}\right)_{C_{\text{I}^-}}$	$\dfrac{RT}{F}\left(\dfrac{\partial \ln i_0}{\partial \Delta\phi_0}\right)_{C_{\text{I}_{\text{I}}^-}}$	$\left(\dfrac{\partial \ln i_0}{\partial \ln C_{\text{I}^-}}\right)_{\Delta\phi_0}$
I-1	$\alpha_{\text{I-1}}$	$\alpha_{\text{I-1}} - \frac{2}{3}$	1
I-2	2	$\frac{2}{3}$	2
I-3	2	0	3
II-1	$\alpha_{\text{II-1}}$	$\alpha_{\text{II-1}} - \frac{2}{3}$	1
II-2	$1 + \alpha_{\text{II-2}}$	$\alpha_{\text{II-2}} - \frac{1}{3}$	2
II-3	2	0	3
III-1	$\alpha_{\text{III-1}}$	$\alpha_{\text{III-1}} - \frac{2}{3}$	1
III-2	$1 + \alpha_{\text{III-2}}$	$\alpha_{\text{III-2}} - \frac{2}{3}$	2

α_i is the transfer coefficient of reaction i. The columns indicate respectively the reaction scheme, the rate-determining step, the theoretical Tafel slope at constant iodide and tri-iodide ion concentrations and the reaction order at the equilibrium potentials.

5. The most probable reaction path for the cathodic reaction

To decide the most probable path for the cathodic reaction, the Tafel slope alone is insufficient, as various reactions may be supported by the experimental Tafel line. Therefore other magnitudes should be considered too, such as the reaction order, the dependence of the degree of coverage on potential and the dependence of half-wave potential on concentration.

Let us first examine the order of reaction with respect to tri-iodide ions. The experimental results satisfy the Frumkin and Tedoradse kinetic method for the rotating disk electrode if the reaction order with respect to tri-iodide ions is 1. If it were 0·5,

the rate equation would yield a linear relationship between i^2 and $i/\omega^{1/2}$, which was not found. A reaction order higher than 1 must obviously be discarded too. Hence, the probable value is 1.

Secondly, we must take into account the dependence of the cathodic half-wave potential on ion concentration. If the cathodic reaction were entirely reversible, the current/potential curve would be described by

$$E_{\text{II-b}} = E_{\text{II-b}}^\circ - \frac{RT}{2F} \ln \frac{\left(1 - \dfrac{i}{(i_{\text{ld}})_{\text{I}^-}}\right)^3}{\left(1 - \dfrac{i}{(i_{\text{ld}})_{\text{I}_3^-}}\right)}, \tag{16}$$

where $(i_{\text{ld}})_i$ is the corresponding limiting current density for the cathodic and anodic processes. According to (16) the half-wave potential should be proportional to the log of the ratio of tri-iodide- to iodide-ion concentrations, as

$$(E_{\text{II-b}})_{1/2} = E_{\text{II-b}}^\circ - \frac{3}{2}\frac{RT}{F} \ln \left[1 - \frac{1}{2}\frac{(i_{\text{ld}})_{\text{I}_3^-}}{(i_{\text{ld}})_{\text{I}^-}}\right] - \frac{RT}{2F} \ln 2. \tag{17}$$

No experimental results fit (17) satisfactorily, since the half-wave potential depends exclusively on the tri-iodide-ion concentration.

Such a dependence however can easily be obtained if a certain degree of irreversibility is considered. In this case the half-wave potential becomes

$$(E_{\text{II-b}})_{1/2} = E_{\text{II-b}}^\circ - \frac{RT}{\alpha_c F} \ln \frac{D_{\text{I}_3^-}}{i_0}. \tag{18}$$

Since according to (18), i_0 is a linear function of the tri-iodide-ion concentration, the dependence of $E_{1/2}$ on log $C_{\text{I}_3^-}$ found in the experiments appears in (18).

From the following considerations, reaction scheme I should be discarded and the discussion centred on schemes II and III, for the cathodic reaction. Let us consider now the following cases:

(i) *Scheme II involving reaction 2 as the rate-determining step.* We have the rate equations

$$(v_{\text{II-2}})_c = (k_{\text{II-2}})_c \bar{C}_{\text{I}_2} C_M \exp\left[-\frac{(\alpha_{\text{II-2}})_c F \Delta\phi}{RT}\right] \tag{19}$$

and

$$(v_{\text{II-2}})_a = (k_{\text{II-2}})_a \bar{C}_{\text{I}^-} C_{M(\text{I})} \exp\left[\frac{(\alpha_{\text{II-2}})_a F \Delta\phi}{RT}\right], \tag{20}$$

where v_i, $\bar{C}_i$, C_i, k_i and α_i are, respectively, the reaction rate of step i for the cathodic (c) and anodic reaction (a), the concentration of i at the metal-solution interphase, the bulk concentration of i, the formal rate constant of step i and its transfer coefficient. If step II-2 is the rate-determining step, the iodine concentration on the electrode surface is regulated by reaction II-3, whose equilibrium constant, $K_{\text{II-3}}$ is

$$K_{\text{II-3}} = \frac{\bar{C}_{\text{I}_2} \bar{C}_{\text{I}^-}}{C_{\text{I}_3^-}}. \tag{21}$$

8

Taking into account (21) in (20), we obtain

$$(v_{\text{II-2}})_c = (k_{\text{II-2}})_c K_{\text{II-3}} \frac{\bar{C}_{\text{I}_3^-}}{\bar{C}_{\text{I}^-}} \, \bar{C}_M \exp\left[-\frac{(\alpha_{\text{II-2}})_c F \Delta\phi}{RT}\right], \tag{22}$$

and the net rate of the cathodic reaction, is

$$v = (v_{\text{II-2}})_c - (v_{\text{II-2}})_a, \tag{23}$$

which in terms of current density is

$$i = zF\left\{(k_{\text{II-2}})_c K_{\text{II-3}} \frac{\bar{C}_{\text{I}_3^-}}{\bar{C}_{\text{I}^-}} \, C_M \exp\left[-\frac{(\alpha_{\text{II-2}})_c F \Delta\phi}{RT}\right]\right.$$
$$\left. - (k_{\text{II-2}})_a \, \bar{C}_{\text{I}^-} C_{M(\text{I})} \exp\left[\frac{(\alpha_{\text{II-2}})_a F \Delta\phi}{RT}\right]\right\}. \tag{24}$$

For negative potentials not too close to the equilibrium potential, (24) yields

$$i = zF(k_{\text{II-2}})_c K_{\text{II-3}} \frac{\bar{C}_{\text{I}_3^-}}{\bar{C}_{\text{I}^-}} \, C_M \exp\left[-\frac{(\alpha_{\text{II-2}})_c F \Delta\phi}{RT}\right], \tag{25}$$

which establishes, at a constant overpotential, a dependence of the rate of reaction on the concentration ratio of tri-iodide to iodide ions which was certainly not encountered. This possibility must therefore be discarded.

(ii) *Scheme III involving reaction 2 as the rate-determining step.* If reaction III-2 is the rds the rate equation is

$$v = (k_{\text{III-2}})_c \bar{C}_{\text{I}_3^-} C_M \exp\left[-\frac{(\alpha_{\text{III-2}})_c F \Delta\phi}{RT}\right] - (k_{\text{III-2}})_a C_{M(\text{I})} \bar{C}_{\text{I}^-}^{-2} \exp\left[\frac{(\alpha_{\text{III-2}})_a F \Delta\phi}{RT}\right] \tag{26}$$

and the corresponding one for reaction III-1 is

$$v = (k_{\text{III-1}})_c C_{M(\text{I})} \exp\left[-\frac{(\alpha_{\text{III-1}})_c F \Delta\phi}{RT}\right] - (k_{\text{III-1}})_a \bar{C}_{\text{I}^-} C_M \exp\left[\frac{(\alpha_{\text{III-1}})_a F \Delta\phi}{RT}\right]. \tag{27}$$

Hence, at high negative overpotentials, the rate of reaction for case (ii) is given by

$$i = F(k_{\text{III-2}})_c \bar{C}_{\text{I}_3^-} C_M \exp\left[-\frac{(\alpha_{\text{III-2}})_c F \Delta\phi}{RT}\right]. \tag{28}$$

If C_M being proportional to the degree of coverage is assumed independent of potential, this equation would support the experimental facts for the cathodic reaction. Besides the first order dependence of i only on $C_{\text{I}_3^-}$, it also comprises the Tafel relationship between potential and current. The constancy of C_M can be demonstrated from several points of view. The number of free sites are proportional to the degree of coverage,

$$C_M = k'\theta_0 = k''(1 - \theta), \tag{29}$$

where θ_0 is the degree of uncovered electrode surface. If θ approaches zero, to a first approximation C_M is constant.

Furthermore, as far as the electrocapillary curve data of solutions containing DMSO are concerned, published results[20] indicate that under the prevailing conditions the greater part of runs were performed at a potential rather far away from the electrocapillary maximum.

Finally, if any type of specific adsorption exists, it is probably an adsorption of the solvent due to its own nature and not to ions present in the solutions or intermediates formed in the course of the electrode reaction.

6. The activation energy of the cathodic reaction

At the equilibrium potential the rate equation (28) becomes

$$i_0 = F(k_{III-2})_c \bar{C}_{I_3} - C_M \exp\left[-\frac{(\alpha_{III-2})_c F \Delta\phi_0}{RT}\right].$$ (30)

On differentiating (30) with respect to $1/T$ and taking into account that the equilibrium potential of the electrochemical system is nil, the experimental activation energy obtained from the temperature dependence of the apparent exchange current density is the activation energy of step III-2, which is very likely the rate-determining step for the cathodic reaction. Then

$$(E_a)_{cat} = 4000 \pm 500 \text{ cal/mole} \approx (E_a)_{III-2}.$$ (31)

7. The most likely reaction path for the anodic reaction. The first wave

As already described, the anodic reaction involves two steps. The first was assigned to oxidation of iodide ion while the second corresponds to oxidation of tri-iodide ion. Both reactions involve a measurable amount of irreversibility, as deduced from the change of the half-wave potential with rotation speed and ionic concentration, although the effect is much larger for the first wave than for the second.

In addition to those facts, the half-wave potentials do not fit the equation predictably for a completely reversible process. Furthermore both waves could be dealt with in terms of the method of intermediate kinetics already mentioned.

Let us first consider again the probable reaction path associated with the first anodic wave by discussing it in terms of the three reaction schemes already mentioned.

(i) If reaction I-1 is rate-determining, the following rate equation emerges,

$$i = F\left\{(k_{I-1})_a C_M \bar{C}_{I^-} \exp\left[\frac{(\alpha_{I-1})_a F \Delta\phi}{RT}\right] - (k_{I-1})_c C_{M(I)} \exp\left[-\frac{(\alpha_{I-1})_c F \Delta\phi}{RT}\right]\right\},$$ (32)

and, as previously postulated, (32) written in terms of the concentration of active sites and at sufficiently high positive overpotentials is

$$i = F(k_{I-1})_a k''(1 - \theta)\bar{C}_{I^-} \exp\left[\frac{(\alpha_{I-1})_a F \Delta\phi}{RT}\right],$$ (33)

and again on the basis of arguments already developed for the cathodic reaction, θ is negligible compared to 1 also in the present case. So, (33) becomes

$$i = F(k_{I-1})_a \bar{C}_{I^-} \exp\left[\frac{(\alpha_{I-1})_a F \Delta\phi}{RT}\right].$$ (34)

On the other hand, if the dependence of the degree of surface coverage on potential is given by

$$1 - \theta = k_\theta \exp\left[-\frac{\alpha_\theta F \Delta\phi}{RT}\right], \tag{35}$$

where K_θ is a proportionality constant and α_θ the transfer coefficient for the degree of coverage, the rate equation is

$$\Delta\phi = K' + \frac{RT}{[(\alpha_{I\text{-}1})_a - \alpha_\theta]F}\ln i \tag{36}$$

where K' involves the log of constant terms. According to (36), the experimental transfer coefficient $(\alpha_1)_a$ should correspond to a difference of $\alpha_{I\text{-}1}$ and α_θ.

(ii) If reaction II-2 is rate-determining, at a low degree of coverage and at high positive overpotential, the rate equation becomes

$$v = (k_{II\text{-}2})_a \bar{C}_{I^-} \exp\left[\frac{(\alpha_{II\text{-}2})_a F \Delta\phi}{RT}\right]. \tag{37}$$

The rate equation for a high degree of coverage, assuming a linear increase of coverage with electrode potential, is for high positive overpotential

$$v = (k_{II\text{-}2})_a K_{II\text{-}1} \bar{C}_{I^-}^{2} \exp\left\{\frac{2(\alpha_{II\text{-}1})_a + (\alpha_{II\text{-}2})_a F \Delta\phi}{RT}\right\}. \tag{38}$$

Predictions of case (ii) are not fulfilled by the experimental data.

(iii) If reaction III-2 is rate-determining, the rate equation obtained for high positive overpotentials is
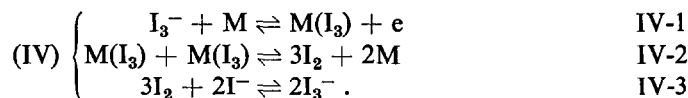
$$v = (k_{III\text{-}2})_a C_{M(I)} \bar{C}_{I^-}^{2} \exp\left[\frac{(\alpha_{III\text{-}2})_a F \Delta\phi}{RT}\right], \tag{39}$$

which also involves a dependence of the current on the square of iodide-ion concentration. Consequently this possibility must also be ruled out.

Finally, the only reaction left as a possible rate-determining step is reaction 1, the only one predicting a first-order dependence of current on iodide-ion concentration. The experimental transfer coefficients, although less than one, are neither 1 nor 0·5 as in apparently simpler cases.

8. *The probable reaction path associated with the second anodic wave*

The interpretation of the second anodic wave is rather restricted because the experimental rate is proportional to tri-iodide-ion concentration and the Tafel slope involves a transfer coefficient of 0·5. As far as this result is concerned, the rate-determining step should be a one-electron per one ion-transfer process. The following reaction scheme which satisfies the foregoing requirements is put forward, if reaction IV-1 is the rds,

$$(IV) \begin{cases} I_3^- + M \rightleftharpoons M(I_3) + e & \text{IV-1} \\ M(I_3) + M(I_3) \rightleftharpoons 3I_2 + 2M & \text{IV-2} \\ 3I_2 + 2I^- \rightleftharpoons 2I_3^- . & \text{IV-3} \end{cases}$$

If IV-1 becomes the rate-determining step, the rate equation at high positive overpotentials and low degree of surface coverage becomes

$$v = (k_{IV\text{-}1})_a \bar{C}_{I_3}\text{-}C_M \exp \left[\frac{(\alpha_{IV\text{-}1})_a \Delta \phi F}{RT} \right].$$ (40)

This equation furnishes the kinetic parameters found experimentally, if it is assumed that $(\alpha_{IV\text{-}1})_a$ is equal to 0·5.

9. *The activation energy of the anodic reactions*

The experimental activation energy for the first wave is 4000 ± 500 cal/mol, and according to the previous discussion, should correspond to the activation energy of reaction I-1.

Accordingly, for the second wave, the experimental activation energy is 3000 ± 500 cal/mol and should be related to reaction IV-1.

10. *Conclusions about the behaviour of iodine–iodide–tri-iodide redox electrode*

The kinetic analysis of the cathodic and anodic processes has yielded different values for the transfer coefficients but as the reactions are part of the same redox process as that deduced from the thermodynamics of the electrode reaction, the sum of the cathodic and anodic transfer coefficients must be equal to one. The results of the present work indicate clearly that this requirement is actually fulfilled:

$$(\alpha)_c + (\alpha_1)_a + (\alpha_2)_a = (0\cdot25 \pm 0\cdot02) + (0\cdot25 \pm 0\cdot05) + (0\cdot50 \pm 0\cdot04) = 1\cdot0 \pm 0\cdot11.$$ (41)

The electrochemical overall reaction comprises the equilibria already known for similar aqueous systems, but an appreciable difference is observed in its kinetics. This particularity should undoubtly be attributed to the nature of the solvent, in which tri-iodide-ion formation is more favoured than in the aqueous system.

Complementary information about this reaction, obtained in a chronopotentiometric study to be published, yields a further support to the interpretation given here to the electrode reactions.

REFERENCES

1. R. T. IWAMOTO, *Analyt. Chem.* **31**, 955 (1959).
2. M. C. GIORDANO, J. C. BAZÁN and A. J. ARVÍA, *Electrochim. Acta*, to be published.
3. M. C. GIORDANO, J. C. BAZÁN and A. J. ARVÍA, in preparation.
4. J. C. BAZÁN and A. J. ARVÍA, *Electrochim. Acta* **10**, 1025 (1965).
5. G. PAUS, to be published.
6. W. E. TRIACA and A. J. ARVÍA, *Electrochim. Acta* **10**, 409 (1965).
7. J. KENTTÄMAA, *Suomen Kemistilehti*, B33, 179 (1960); P. G. SEARS, G. R. LESTER and L. R. DAWSON, *J. phys. Chem.* **60**, 1433 (1956).
8. R. S. DRAGO, B. WAYLAND and R. L. CARLSON, *J. Am. chem. Soc.* **85**, 3125 (1963); F. AUGDAHL and P. KLAEBOE, *Acta chem. scand.* **18**, 27 (1964); P. KLAEBOE, *Acta chem. scand.* **18**, 27 (1964).
9. M. C. GIORDANO, J. C. BAZÁN and A. J. ARVÍA, *J. inorg. nucl. Chem.* in press.
10. B. G. LEVICH, *Physico-chemical Hydrodynamics*, Chap. 2. Prentice-Hall, Englewood Cliffs, N. J. (1962).
11. G. CHARLOT, G. BADOZ-LAMBLING and B. TRÉMILLON, *Electrochemical Reactions*. Elsevier, Amsterdam (1962).

12. B. MUSULIN, W. J. JONES and M. J. BLEEM, *J. inorg. nucl. Chem.* **26,** 239 (1964).
13. K. J. VETTER, *Z. phys. Chem.* **199,** 22 (1952); **199,** 285 (1952).
14. G. EDGAR and S. H. DIGGS, *J. Am. chem. Soc.* **38,** 256 (1916).
15. J. D. NEWSON and A. C. RIDDIFORD, *J. electrochem. Soc.* **108,** 695, 699 (1961).
16. R. E. POWELL, W. ROSEVEARE and H. EYRING, *Ind. Engng. Chem.* **33,** 430 (1941).
17. A. FRUMKIN and G. TEDORADSE, *Z. Elektrochem.* **62,** 251 (1958).
18. H. A. VIDELA and A. J. ARVÍA, *Electrochim. Acta,* **10,** 21 (1965).
19. J. O'M. BOCKRIS, *Modern Aspects of Electrochemistry*, No. 1, Chap. 4. Butterworths, London (1955).
20. I. M. KOHLTOFF and T. B. REDDY, *J. electrochem. Soc.* **108,** 980 (1961).